Preparation and Physicochemical, Structural and Morphological Characterization of Phosphorylated Starch

Natan da Silva Miranda Sechi[a]*, Patricia Teixeira Marques[a]

[a] Department of Chemistry, Federal University of Technology, Pato Branco, PR, Brazil

Phosphorylation of starch has resulted in appreciated material properties for applications in drug matrices. This study aimed to obtain and characterize samples of phosphorylated starch with sodium trimetaphosphate (STMP) and sodium tripolyphosphate (STPP). SEM micrographs allowed evidence that in relation to the starch in natura, the samples showed a loss of grain form in addition to formation of particle agglomerates. X-ray diffractograms of these samples indicated amorphization process, with modifications of the peaks in the region between 15 and 20 º 2θ. FTIR spectra of phosphorylated samples showed variations and new bands related to phosphorylation. Through of methylene blue adsorption isotherms it was observed better adjustment adsorptions on phosphorylated sample to Freundlich model. The new biomaterials showed adsorptive capacity of model cationic nature drug, demonstrate potentiality to application in controlled release systems.

Keywords: *solubility, degree substitution, cationic adsorbate*

1. Introduction

Starches in natura present some limitations in some types of industrial processes and technological applications. This can be reversed using chemical modification methods[1,2]. Using microwave radiation with lipases, esterification with lipase, formation of hydrogels by photopolymerization in UV radiation, esterification with ferulic acid, ozone oxidation, phosphorylation are among the modification methods used[3]. Phosphorylation modification process, corresponding to insertion of phosphate groups, generate starches with differentiated properties, such as modification in solubility, pulp properties and morphology[4-6]. The process of phosphorylation of starches has been realized by different methods and phosphorylation agents. Among the phosphorylation agents, the Sodium Trimetaphosphate (STMP) and Sodium Tripolyphosphate (STPP) salts are characterized by their low cost, capacity to obtain materials with controlled substitution degrees, modifications in physicochemical properties even with degrees of low substitution and few changes in the base structure of starch chains. The process of phosphorylation with STMP and STPP can, depending on the reaction conditions, produce new differentiated materials such as monostarch monophosphate or distarch monophosphate, both with anionic character from the phosphate groups[7,8]. Starch phosphorylation with STMP has been studied and demonstrated by Sang, Prakash and Seib (2007)[9] who concluded that the products are predominantly diesterified and may contain phosphate mono and triesters in lesser amounts. The authors also evaluated starch phosphorylation

with STPP and observed predominance of monoesterified products, also with minority presence of phosphate diesters. These observations were obtained by means of ^{31}P nuclear magnetic resonance (NMR) spectroscopy, a technique that also allowed the detection of free inorganic phosphorus residues. The reactions of starch phosphorylation with STMP and STPP with the major products, based in Sang, Prakash and Seib (2007)[9], are shown in figure 1.

Phosphorylated starches have been shown to be promising materials for acting as a matrix for controlled drug delivery systems[10,11]. Also, various technological applications of the starches can be improved with phosphorylated products, because the modification of various properties such as increase of paste clarity, viscosity and water absorption capacity can be achieved[4,12]. The objectives of the present study were to obtain phosphorylated starches with different phosphate reagents, STMP and STPP, and to evaluate their structural, chemical and surface properties, compared with original starch.

2. Materials and Methods

2.1. Materials

In this work, was used comercial soluble starch P.A. A.C.S., labeled solubility of 5 g L^{-1} (Dinâmica Química Contemporânea - Diadema, Brazil), sodium tripolyphosphate and sodium trimetaphosphate were obtained from ICL Brazil (São Paulo, Brazil), anhydrous sodium sulfate (Vetec - Duque de Caxias, Brazil), sodium hydroxide (Vetec - Duque de Caxias, Brazil), concentrated hydrochloric acid (Alphatec - Brazil) and etanol 99% (Alphatec - Brazil). For characterization,
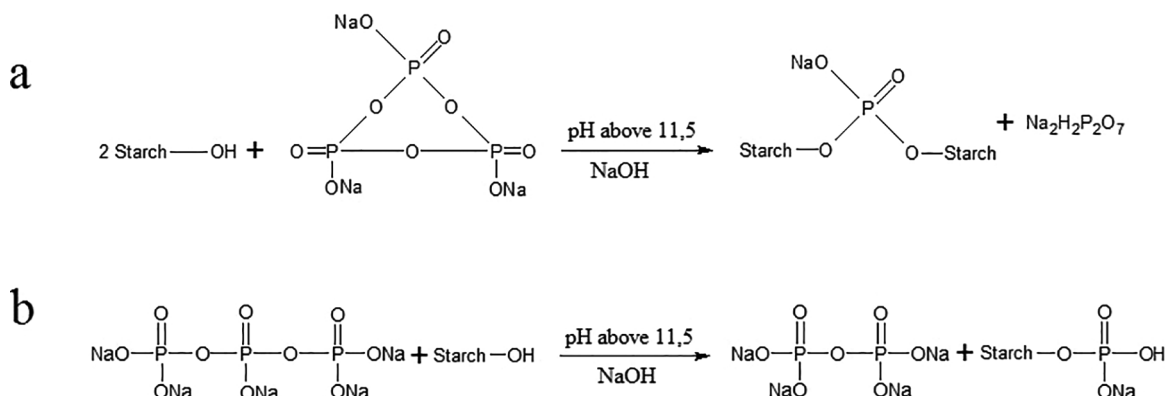
Figure 1. Propositions of Starch Phosphorylation Reactions with (a) STMP and (b) STPP in alkaline medium.

analytical grade reagents were used, anhydrous monobasic potassium phosphate (Synth - Diadema, Brazil), ammonium vanadate and ammonium molybdate (Vetec - Duque de Caxias, Brazil), nitric acid P.A. 65% (Proquimios - Rio de Janeiro, Brazil) and Methylene Blue (Industrial Chemical Group - Essex, United Kingdom).

2.2. Obtained phosphorylated starches

Samples of modified starch were obtained based on the methods employed by Cury, Klein and Evangelista (2008)[13] and Soares et al. (2013)[14], with modifications. 10 g of starch were dispersed in 200 ml of distilled water, then 0.5 g of sodium sulfate were dissolved and the pH was adjusted to 9.0 with addition of sodium hydroxide 1 mol L^{-1}. The suspension was pre-heated to approximately 70 ºC under constant stirring. 3 g of modifying agent (STMP or STPP) was added and the pH was again adjusted to 9 with sodium hydroxide 1 mol L^{-1}. Modification reaction was conducted under constant stirring at room temperature for 2 hours and terminated by lowering the pH to 6 with addition of hydrochloric acid 25% (v/v). Washing was performed with 130 ml of ethanol A.P. and then the samples were vacuum filtered and oven dried at 60 ºC for 48 hours.

The samples were named ST, ST-TP and ST-TM, corresponding to the in natura starch, STPP-modified starch and STMP-modified starch, respectively.

2.3. Characterization by Fourier Transform Infrared (FTIR) spectroscopy

The (FTIR) spectroscopic analyzes were performed using the KBr pellets method. The pellets were obtained by mixing sample portions and KBr pressed at 80 kgf m^{-2}. Readings were performed in the range of 400 to 4000 cm^{-1}, with resolution of 2 cm^{-1} and 32 scans in FTIR spectrometer (Perkin Elmer, Frontier model, USA).

2.4. [31]P Nuclear Magnetic Resonance (NMR) spectroscopy

^{31}P NMR spectra were obtained on NMR spectrometer (Bruker Avance III HD 400 WB, USA) by solid state resonance. Pure solid samples were analyzed without any treatment. The spectrometer was configured for frequency analysis of 161.67 MHz at room temperature, using a double resonance probe with CP/MAS detection system.

2.5. Water Solubility

Solubility of the samples was determined in triplicate, based on Kagimura et al. (2015)[15] with modifications. 20 mg of sample were added to 20 ml of distilled water, remained constant stirring for 24 h at 150 rpm and 25 ºC. It was then centrifuged at 18,000 x g for 15 min, the supernatant was collected and the starch concentration was determined by the phenol-sulfuric method[16].

2.6. Degree of Substitution (DS)

Degree of substitution was determined according to Passauer, Bender and Fischer (2010)[17] with modifications. First the phosphorus contents of the samples were determined by spectrophotometric colorimetry, according to vanadium-molybdate standard method, using spectrophotometer (Thermo Scientific, Evolution 60S model, USA). Samples were calcined at 575 ºC for 4 hours, after cooling 4 mL of hydrochloric acid 16.67% (v/v) were added, the volumes were completed with distilled water up to 100 mL and filtered on filter paper. In test tubes were added 1 mL of filtered sample, 5 mL of distilled water and 1 mL of vanadium-molybdate reagent (mixture of equal volumes of 25% ammonium molybdate and 25% ammonium vanadate acidified with 4.3% (v/v) of nitric acid). After 45 minutes of rest, the spectrophotometric readings were carried out at 420 nm. As a phosphorus standard, the

monobasic potassium phosphate salt was used. The degrees of substitution (DS) were calculated by means of equation A.

$$DS = \frac{162 \times P\%}{3100 - 102 \times P\%} \quad (A)$$

In equation A, 162 corresponds to the molecular weight of the monomeric starch unit, P% to the phosphorus content obtained by colorimetry, number 3100 refers to the molecular weight of the phosphorus multiplied by 100 and 102 corresponds to the mass of the monophosphate substituent group.

2.7. Morphological Analysis by Scanning Electron Microscopy (SEM)

Samples were characterized morphologically by scanning electron microscopy (SEM). The micrographs were captured on a benchtop microscope (Hitachi, model TM3000, Japan), suitable for analysis of biological samples, configured at 15 kV, with approximations in the range of 300 to 800 x and with specimens fixed to carbon ribbons and without coating.

2.8. X-Ray diffraction

Diffraction patterns of the samples were obtained using an X-ray diffractometer (Rigaku, model MiniFlex 600, Japan), configured with copper lamp radiation (CuKα = 1.5418 Å), 40 kV and 15 mA. The diffractograms were generated with readings in the range of 10 to 60 ° 2θ, step of 0.02 ° 2θ and velocity of 5 ° 2θ min^{-1}.

2.9. Methylene blue adsorption isotherm

In Falcon plastic tubes, 10 mL of methylene blue solutions were added with concentrations ranging from 0.25 to 4 mg L^{-1} and then 20 mg of sample was added in each tube. Under shelter from the light the adsorption experiment was conducted at 30 °C, under agitation of 155 rpm for 24 hours in a rotational incubator. The mixture was centrifuged for 30 minutes at 5000 x g and the supernatant separated for spectrophotometer reading (Thermo Scientific, model Evolution 60S, USA) at 600 nm wavelength. The calibration curve of methylene blue was constructed with data of concentrations between 0.1 and 5 mg L^{-1}.

3. Results and Discussion

3.1. FTIR spectroscopy

FTIR spectra of the samples ST, ST-TP and ST-TM are shown in figure 2. In the 2800-3000 cm^{-1} region similar bands were observed in all samples corresponding to the C-H stretch, common of glycosidic structures[18].

Also, bands common to all samples in the 1654 cm^{-1} regions of the O-H flexion were observed by the presence of water[19], at 762 cm^{-1} attributed to C-C stretch, at 1162 cm^{-1} and 1085 cm^{-1} attributed to C-O and C-C bonds, related to elongation in the C-O-C group of the hexose ring[20] and in 993 and 930 cm^{-1} attributed to the C-OH and CH_2 deformations characteristic of starch molecules[18,21].
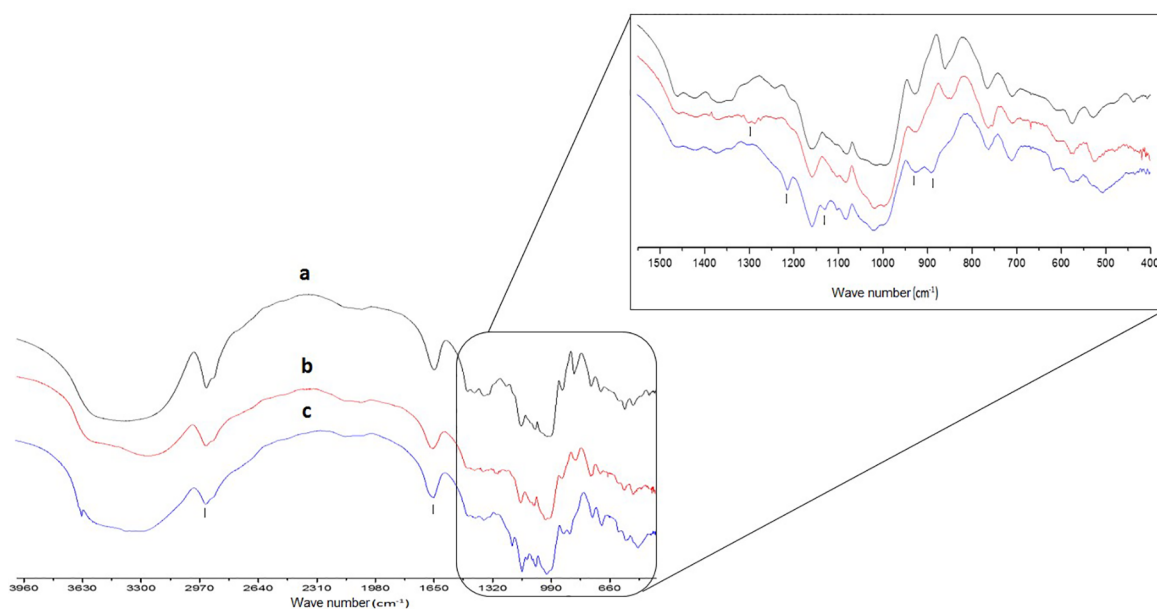
Figura 2. FTIR absorption spectra of samples (a) ST (b) ST-TM and (c) ST-TP.

In the ST-TM sample spectrum, small intensity variations were observed in some bands in relation to the ST spectrum, as well as a new low intensity band in the 1300 cm^{-1} region that can be associated with water present in the material[22], however specific bands of bound phosphate groups were not perceptible, probably due to the reduced number of phosphate introduced, as already reported by Li et al. (2009)[23]. On the other hand, the spectrum of the ST-TP sample presented, in addition to small variations in intensity, a new band at 3630 cm^{-1} associated with O-H stretching of unbound water, probably adsorbed on the surface of the sample[24,25], a band at 1214 cm^{-1} assigned to symmetrical stretching P=O[19,20], a band at 1129 cm^{-1} related to symmetrical and asymmetrical stretching of the PO_2 group[26] and a band at 889 cm^{-1} may be related with the P-O bond[27]. Such alterations in the absorption in the infrared region, evidenced the occurrence of the phosphorylation process, especially for the spectra of the ST-TP sample.

3.2. ^{31}P (NMR) spectroscopy

^{31}P NMR spectra of the ST-TP and ST-TM samples are shown in figure 3, with the respective structures formed, the starch molecule in the figures is represented by (St). Spectrum ST-TM sample (Figure 3a) showed two groups of signals in the range of 15 to -20 ppm. The signals between δ -1.8 and -5 ppm are attributed to the presence of distarch monophosphate (DSMP)[9]. The DSP structure derives from the phosphorylation of starch by STMP at pH above 8, according to the mechanism proposed by Lim e Seib (1993)[28]. Other signals between δ -5 and -10 ppm may be attributed to monostarch diphosphate formation (MSDP), as observed by Passauer, Bender e Fisher (2010)[17].

^{31}P NMR spectrum of the ST-TP sample (Figure 3b) showed two signals in δ 3.6 and 1.6 ppm related to obtaining monostarch monophosphate (MSMP) and DSMP structures respectively[12,17,29]. The MSMP structure is characterized by grouping phosphate bound through ester bond with the C6 carbon of the glycosidic unit of starch[9,17]. Two signals presented between δ -5 and -10 ppm in the ST-TP sample spectrum are attributed to MSDP formation, as observed for the ST-TM sample.

3.3. Water solubility

Table 1 shows the water solubility data of samples ST, ST-TP and ST-TM. The ST sample showed low solubility, forming a more turbid suspension with fine particles, common to this type of material[30]. The ST-TP and ST-TM modified samples showed increases in solubility which may be related to the greater swelling power, because with certain levels of phosphate insertion the water penetration into the starch granules is increased and consequently the swelling can be facilitated, also may be related to the partial gelatinization
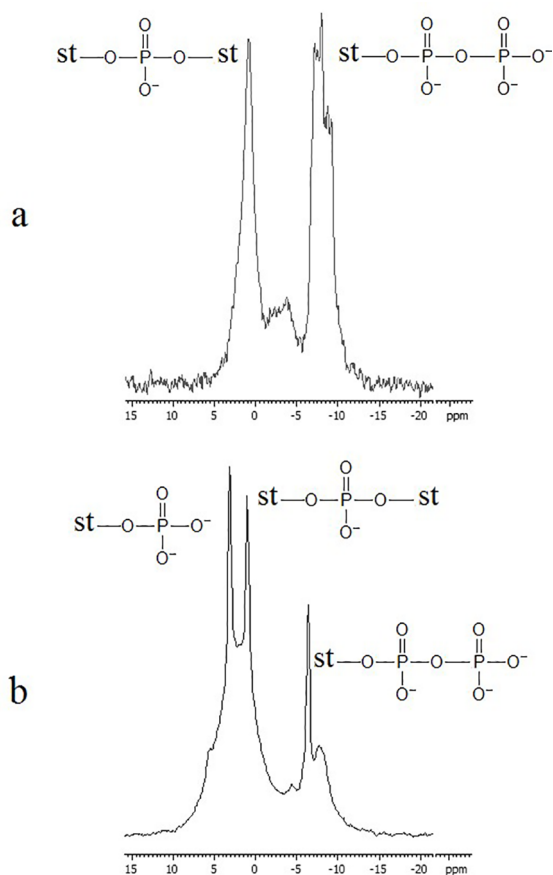
Figura 3. ^{31}P NMR spectra of samples (a) ST-TM and (b) ST-TP.

Table 1. Water Solubility.

Sample	Solubility % (w/w)
ST	3,06 ± 1,89
ST-TP	43,47 ± 0,65
ST-TM	39,67 ± 0,89

process of the starch, even though sodium sulphate is used to delay this process[30,31].

In phosphorylated starches with crosslinking process, a direct relation of swelling power and solubility is generally observed, so that at low crosslinking levels there is an increase in these properties, but at very high crosslinking levels the leaching of starch molecules into water is difficult and swelling and solubility are reduced[31,32].

3.4. Degree of Substution (DS)

The degrees of substitution of the samples are presented in table 2. The ST sample did not present phosphorus content, which is in agreement with the expected. The ST-TP and ST-TM samples presented low levels of phosphorus, however, sufficient to cause changes in several starch properties, as observed by Stahl et al. (2007)[4].

Table 2. Degree of substitution.

Sample	Phosphorous Content (%)	Degree of Substitution Phosphate
ST	-	-
ST-TP	0,220	0,0115
ST-TM	0,067	0,0035

ST-TP showed a higher degree of substitution, which may justify its greater solubility and larger changes modifications in the absorptions in the infrared region. Wongsagonsup et al. (2005)[6] obtained similar results, with phosphorylated starch samples with STPP presenting values much higher of degree of substitution than phosphorylated samples with STMP.

3.5. Scanning Electron Microscopy (SEM)

Morphological characterization of samples ST, ST-TP and ST-TM was performed by means of the micrographs presented in figure 4.

The ST sample presented elliptical and ellipsoidal grain morphology, with more homogeneous sizes as expected for this type of material, without modifications in the granule structure[23]. The samples ST-TP and ST-TM, in turn, presented loss of grain format. Their surfaces became rough, porous and irregular and agglomerations of granules were observed which provided an increase in particle sizes. Such agglomerations may be related to the phosphorylation process[5], whose insertion of the phosphate groups has modified the intermolecular interactions between the starch chains, and also the effect of the granule rupture in the fractions possibly gellled.

3.6. X-Ray diffraction

The X-ray diffractograms of the samples ST, ST-TP and ST-TM are shown in figure 5. ST presented diffraction pattern similar to those commonly found in type A starches, mostly composed of cereal starches, which have a three-dimensional configuration of double helices of amylose and amylopectin[33,34].

The phosphorylated ST-TP and ST-TM samples showed different diffraction patterns from the starting sample, ST, evidenced by the suppression of the main ST peaks at 15, 17 and 23 ° 2θ. This characteristic is due to the amorphization process undergone by the starch, associated to insertion of new groups at non-periodic intervals along the starch chains, which causes a more random spatial distribution, the possible structural rearrangement resulting from alkalinization in the previous process to reaction with the phosphates and also the presence of partial gelling[14,35].

ST-TP presented small new peaks in the regions of 26, 29 and 31 ° 2θ, which may be related to changes in three-dimensional network of the chains, attributed to formation of DSMP (crosslinking process)[35].

3.7. Methylene blue adsorption isotherm

Preliminary methylene blue adsorption tests on the ST-TP and ST-TM samples presented better results for the Freundlich adsorption model according to the R^2 coefficients shown in table 3. The Langmuir isotherms data presented a very large randomness, this non-linear behavior suggests that the adsorption does not behave in a similar way to the model proposed by Langmuir, at least under the conditions studied.
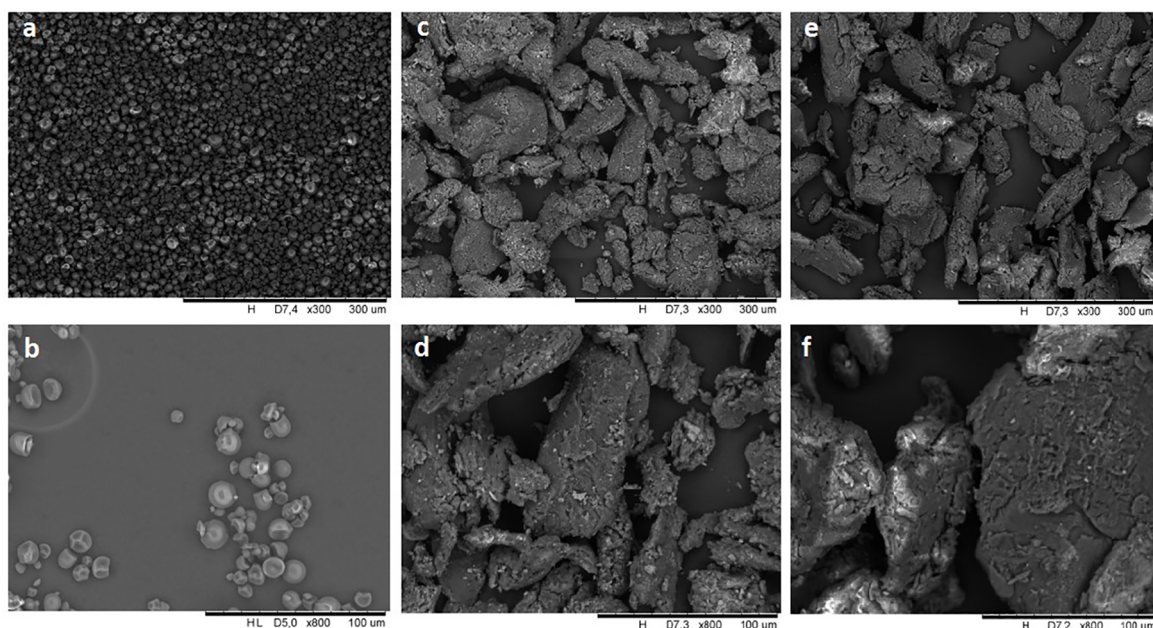
Figure 4. Micrographs with approximations of the samples (a) ST 300x (b) ST 800x (c) ST-TP 300x (d) ST-TP 800x (e) ST-TM 300x and (f) ST-TM 800x.
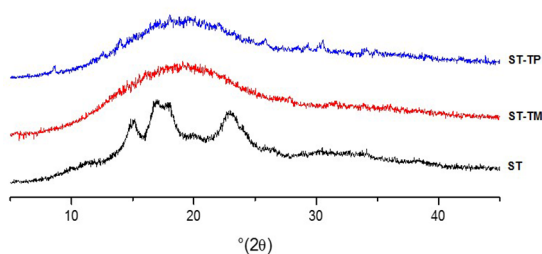
Figure 5. Diffractograms of ST, ST-TM and ST-TP samples.

Table 3. Methylene blue adsorption isotherms data on the phosphorylated samples, using Langmuir and Freundlich models.

	Langmuir			Freundlich		
	Q (mg g^{-1})	K (L mg^{-1})	R^2	Kf (L g^{-1})	n	R^2
ST-TP	0,568	0,748	0,311	1,390	0,640	0,875
ST-TM	1,620	0,226	0,677	0,278	1,228	0,9843

Sample ST showed very low, undetectable methylene blue adsorption, therefore, the data were not reported.

A larger study should be carried out to better understand the adsorption mechanism. However, it is possible to observe that the ST-TP sample presented adsorption potential higher than the ST-TM sample, Which suggests that its structure and surface were more strongly altered, which is in accordance with the results of FTIR spectroscopy, solubility and phosphorus content and that may be related to the increase of the anionic character of the material surface due to the insertion of the phosphate and also to the rupture of granule with an apparent increase in theroughness and porosity of the surfaces observed in micrographs obtained by SEM. This achievement of adsorptive potential in the phosphorylated samples suggests that they are promising for application in drug delivery systems, where they could act as a vehicle for cationic active principles.

4. Conclusions

Starch phosphorylation process has been successfully performed according to the degree of substitution data, ^{31}P NMR spectra and FTIR absorptions observed. The phosphorylated materials presented increased solubility, structural and morphological changes and amorphous diffraction patterns. The adsorptive properties were higher in the phosphorylated starches, with higher adsorption capacity for the sample with higher DS. These data may indicate prospecting in the application as biodegradable adsorbents of cationic adsorbents as the model adsorbent used, methylene blue. Confirmed their respective modifications, the phosphorylated starches will be further studied on new properties and applications.

5. Acknowledgements

6. References

1. Gao F, Li D, Bi C, Mao Z, Adhikari B. Preparation and characterization of starch crosslinked with sodium trimetaphosphate and hydrolyzed by enzymes. *Carbohydrate Polymers*. 2014;103:310-318. DOI: 10.1016/j.carbpol.201 3.12.028

2. Chatakanonda P, Varavinit S, Chinachoti P. Effect of Crosslinking on Thermal and Microscopic Transitions of Rice Starch. *LWT - Food Science and Technology*. 2000;33(4):276-284. DOI: 10.1006/fstl.2000.0662

3. Kaur B, Ariffin F, Bhat R, Karim AA. Progress in starch modification in the last decade. *Food Hydrocolloids*. 2012;26920:398-404. DOI: 10.1016/j.foodhyd.2011.02.01 6

4. Stahl JA, Lobato LP, Bochi VC, Kubota EH, Gutkoski LC, Emanuelli T. Physicochemical properties of Pinhão (Araucaria angustifolia, Bert, O. Ktze) starch phosphates. *LWT - Food Science and Technology*. 2007;40(7):1206-1214. DOI: 10.1016/j. lwt.2006.07.015

5. Singh AV, Nath LK. Synthesis and evaluation of physicochemical properties of cross-linked sago starch. *International Journal of Biological Macromolecules*. 2012;50(1):14-18. DOI: 10.1016/j. ijbiomac.2011.09.003

6. Wongsagonsup R, Shobsngob S, Oonkhanond B, Varavinit S. Zeta Potential (ζ) and Pasting Properties of Phosphorylated or Crosslinked Rice Starches. *Starch*. 2005;57(1):32-37. DOI: 10.1002/star.200400311

7. Manoi K, Rizvi SSH. Physicochemical characteristics of phosphorylated cross-linked starch produced by reactive supercritical fluid extrusion. *Carbohydrate Polymers*. 2010;81(3):687-694. DOI: 10.1016/j.carbpol.2010.03.042

8. Carmona-Garcia R, Sanchez-Rivera MM, Méndez-Montealvo G, Garza-Montoya B, Bello-Pèrez LA. Effect of the cross-linked reagent type on some morphological, physicochemical and functional characteristics of banana starch (*Musa paradisiaca*). *Carbohydrate Polymers*. 2009;76(1):117-122. DOI: 10.1016/j. carb pol.2008.09.029

9. Sang Y, Prakash O, Seib PA. Characterization of phosphorylated cross-linked resistant starch by ^{31}P nuclear magnetic resonance (^{31}P NMR) spectroscopy. *Carbohydrate Polymers*. 2007;67(2):201-212. DOI: 10.1016/j.carbpol.2006.05.009

10. O'Brien S, Wang YJ. Effects of shear and pH on starch phosphates prepared by reactive extrusion as a sustained release agent. *Carbohydrate Polymers*. 2009;77(3):464-471. DOI: 10.1016/j. carbpol.2009.01.014

11. Fang YY, Wang LJ, Li D, Li BZ, Bhandari B, Chen XD, et al. Preparation of crosslinked starch microspheres and their drug

loading and releasing properties. *Carbohydrate Polymers*. 2008;74(3):379-384. DOI: 10.1016/j.carbpol.2008.03.005

12. Polnaya FJ, Haryadi, Marseno DW, Cahyanto MN. Effects of phosphorylation and cross-linking on the pasting properties and molecular structure of sago starch. *International Food Research Journal*. 2013;20(4):1609-1615.

13. Cury BSF, Klein SI, Evangelista RC. Modeling a system of phosphated cross-linked high amylose for controlled drug release. Part 1: Synthesis and polymer characterization. *Reactive and Functional Polymers*. 2008;68(8):1200-1206. DOI: 10.1016/j.reactfunctpolym.2008.04.003

14. Soares GA, Castro AD, Cury BSF, Evangelista RC. Blends of cross-linked high amylose starch/pectin loaded with diclofenac. *Carbohydrate Polymers*. 2013;91(1):135-142. DOI: 10.1016/j.carbpol.2012.08.014

15. Kagimura FY, Cunha MAA, Theis TV, Malfatti CRM, Dekker RFH, Barbosa AM, et al. Carboxymethylation of (1 → 6)-β-glucan (lasiodiplodan): Preparation, characterization and antioxidant evaluation. *Carbohydrate Polymers*. 2015;127:390-399. DOI: 10.1016/j.carbpol.2015.03.045

16. DuBois M, Gilles KA, Hamilton JK, Rebers PA, Smith F. Colorimetric Method for Determination of Sugars and Related Substances. *Analytical Chemistry*. 1956;28(3):350-356. DOI: 10.1021/ac60111a017

17. Passauer L, Bender H, Fischer S. Synthesis and characterisation of starch phosphates. *Carbohydrate Polymers*. 2010;82(3):809-814. DOI: 10.101 6/j.carbpol.2010. 05.050

18. Lima BNB, Cabral TB, Neto RPC, Tavares MIB, Pierucci APT. Estudo do amido de farinhas comerciais comestíveis. *Polímeros*. 2012;22(5):486-490. DOI: 10.1590/S0104-14282012005000062

19. Suflet DM, Nicolescu A, Popescu I, Chitanu GC. Phosphorylated polysaccharides. 3. Synthesis of phosphorylated curdlan and its polyelectrolyte behaviour compared with other phosphorylated polysaccharides. *Carbohydrate Polymers*. 2011;84(3):1176-1181. DOI: 10.1016/j.carbpol.2011.01.010

20. Shi A, Li D, Wang L, Zhou Y, Adhikari B. Spray drying of starch submicron particles prepared by high pressure homogenization and mini-emulsion cross-linking. *Journal of Food Engineering*. 2012;113(3):399-407. DOI: 10.1016/j.jfoodeng.2012.06.017

21. Rocha DA, Abreu CMP, Cardoso MG, Corrêa AD, Contado EWNF. Obtenção e caracterização físico-química e química do polvilho da fruta-de-lobo (Solanum lycocarpum A. St-Hil). *Scientia Plena*. 2012;8(9):099909-1.

22. Luo FX, Huang Q, Fu X, Zhang LX, Yu SJ. Preparation and characterisation of crosslinked waxy potato starch. *Food Chemistry*. 2009;115(2):563-568. DOI: 10.1016/j.foodchem.2008.12.052

23. Li B, Wang L, Li D, Chiu YL, Zhang Z, Shi J, et al. Physical properties and loading capacity of starch-based microparticles crosslinked with trisodium trimetaphosphate. *Journal of Food Engineering*. 2009;92(3):255-260. DOI: 10.1016/j.jfoodeng.2008.10.008

24. Hernandez-Soriano MC, Kerré B, Kopittke PM, Horemans B, Smolders E. Biochar affects carbon composition and stability in soil: a combined spec troscopy-microscopy study. *Scientific Reports*. 2016;6:25127. http://dx.doi.org/10.1038/srep25127

25. Zhang S, Guan Y, Fu GQ, Chen BY, Peng F, Yao CL, et al. Organic/Inorganic Superabsorbent Hydrogels Based on Xylan and Montmorillonite. *Journal of Nanomaterials*. 2014;2014:1-11. DOI: 10.1155/2014/675035

26. Dai L, Qi YP, Niu LN, Liu Y, Pucci CR, Looney SW, et al. Inorganic-Organic Nanocomposite Assembly Using Collagen as a Template and Sodium Tripolyphosphate as a Biomimetic Analog of Matrix Phosphoprotein. *Crystal Growth & Design*. 2011;11(8):3504-3511. DOI: 10.1021/cg200663v

27. Shi F, Shi J, Li Y. Mechanochemical Phosphorylation and Solubilisation of β-D-Glucan from Yeast Saccharomyces cerevisiae and Its Biological Activities. *PLoS ONE*. 2014;9(7):e103494. DOI: 10.1371/journal.pone.0103494

28. Lim S, Seib PA. Preparation and Pasting Properties of Wheat and Corn Starch Phosphates. *Cereal Chemistry*. 1993;70(2):137-144.

29. Zhao J, Chen Z, Jin Z, Waard P, Buwalda P, Gruppen H, et al. Level and position of substituents in cross-linked and hydroxypropylated sweet potato starches using nuclear magnetic resonance spectroscopy. *Carbohydrate Polymers*. 2015;131:424-431. DOI: 10.1016/j.carbpol.2015.06.005

30. Singh N, Singh J, Kaur L, Sodhi NS, Gill BS. Morphological, thermal and rheological properties of starches from different botanical sources. *Food Chemistry*. 2003;81(2):219-231. DOI: 10.1016/S0308-8146(02)00416-8

31. Wongsagonsup R, Pujchakarn T, Jitrakbumrung S, Chaiwat W, Fuongfuchat A, Varavinit S, et al. Effect of cross-linking on physicochemical properties of tapioca starch and its application in soup product. *Carbohydrate Polymers*. 2014;101:656-665. DOI: 10.1016/j.carbpol.2013.09.100

32. Koo SH, Lee KY, Lee HG. Effect of cross-linking on the physicochemical and physiological properties of corn starch. *Food Hydrocolloids*. 2010;24(6-7):619-625. DOI: 10.1016/j.foodhyd.2010.02.009

33. Hizukuri S. X-Ray Diffractometric Studies on Starches. Part VI Crystalline Types of Amylodextrin and Effect of Temperature and Concentration of Mother Liquor on Crystalline Type. *Agricultural and Biological Chemistry*. 1961;25(1):45-49. DOI: 10.1080/00021369.1961.10857772

34. Vazquez A, Cyras VP, Alvarez VA, Moran JI. Starch/Clay Nano-Biocomposites. In: Avérous L, Pollet E, eds. *Environmental Silicate Nano-Biocomposites*. London: Springer London; 2012. p. 287-321.DOI: 10.1007/978-1-4471-4108-2_11

35. Carbinatto FM, Castro AD, Cury BSF, Magalhães A, Evangelista RC. Physical properties of pectin-high amylose starch mixtures cross-linked with sodium trimetaphosphate. *International Journal of Pharmaceutics*. 2012;423(2):281-288. DOI: 10.1016/j.ijpharm.2011.11.042